上海交通大学 SHANGHAI JIAO TONG UNIVERSITY

Autonomous Robot Lab 自主机器人实验室

SJTU

Submitted for IROS 2021

A Steerable Cross-axis Notched (SCAN) Continuum Manipulator

Yilin Cai, Xiaojie Ai, Anzhu Gao, Member, IEEE,
and Weidong Chen, Member, IEEE

2021.3.25

饮 水 思 源 • 爱 国 荣 校

1. Background: Continuum Robots for Surgeries

Bronchoscopy

cable-driven continuum robot

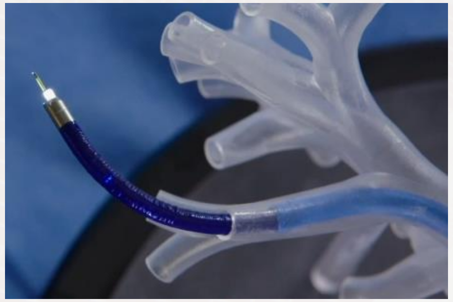

Monarch ™ System (Auris Health)

Abdominal Surgery

Multi-backbone, concentric tubes

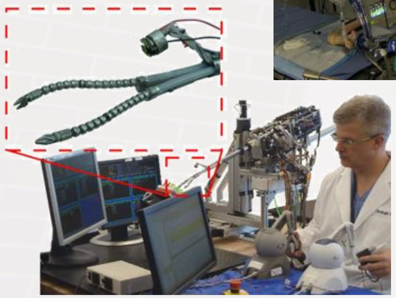

A.Bajo 2012

Flex Robotic System

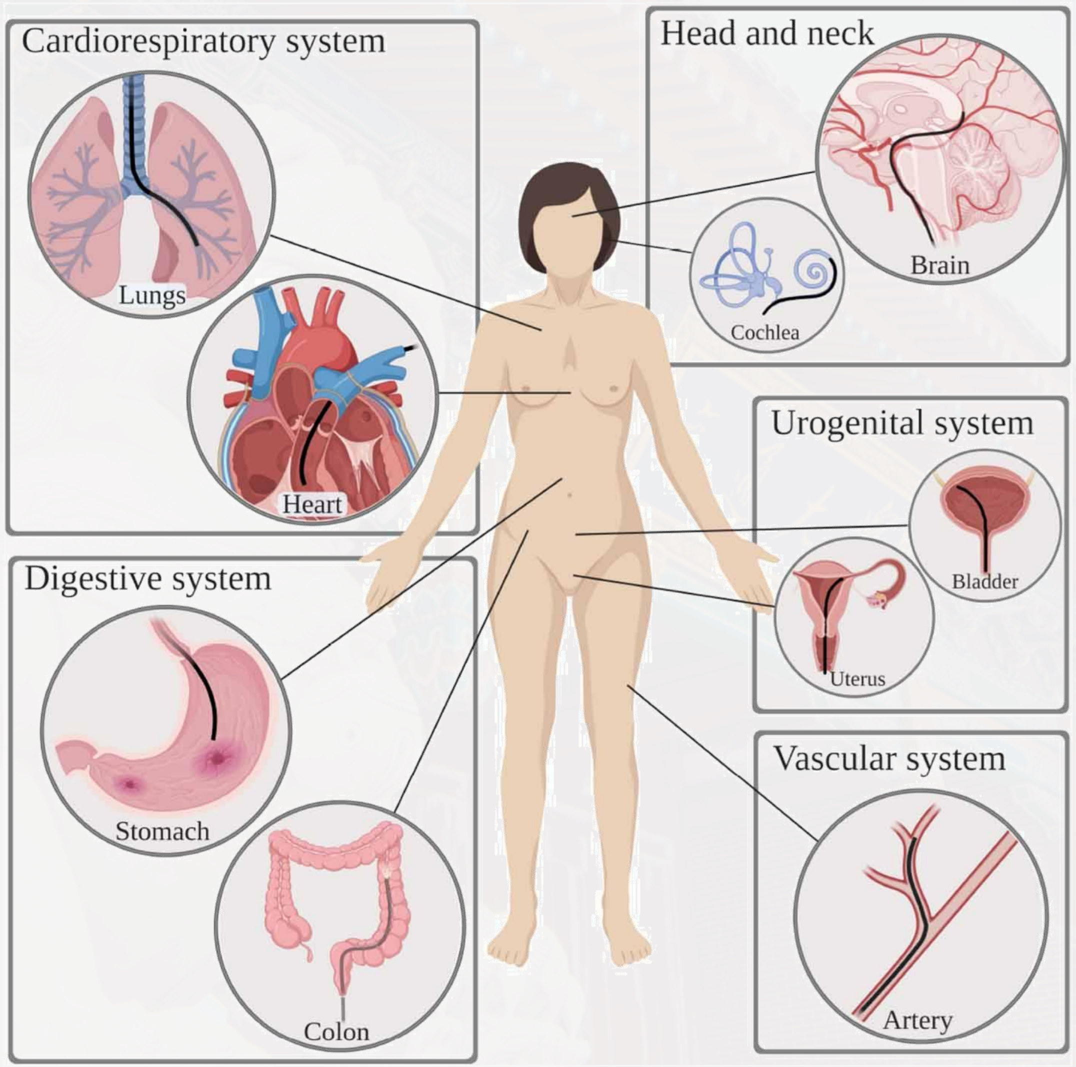

Neurosurgery

Steerable needle, concentric tubes

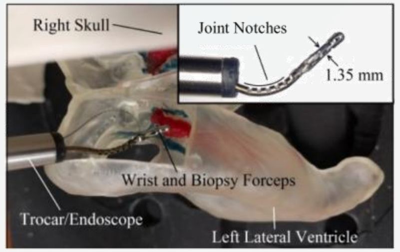

K. Eastwood 2016 ICRA

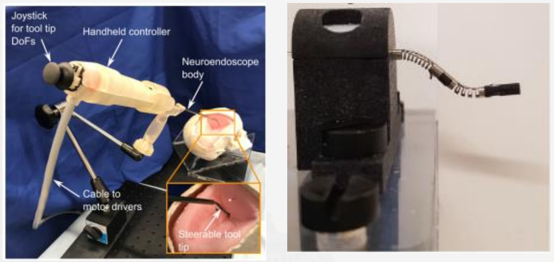

Y. Chitalia 2020

Urologic Surgery

Multi-backbone, concentric tubes

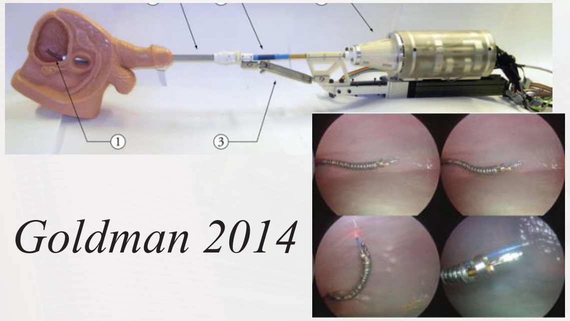

R. Goldman 2014

1. Background: Notched Continuum Manipulator

Notched-tube compliant mechanisms

Uni-directional **Bi-directional**

Asymmetric **Symmetric**

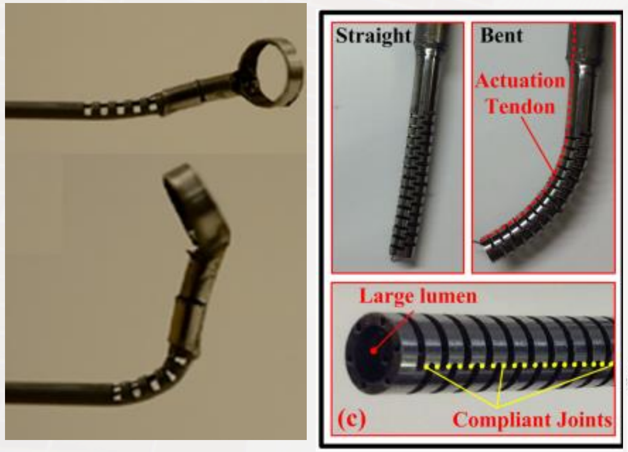

[York 2015] [Gao 2017]

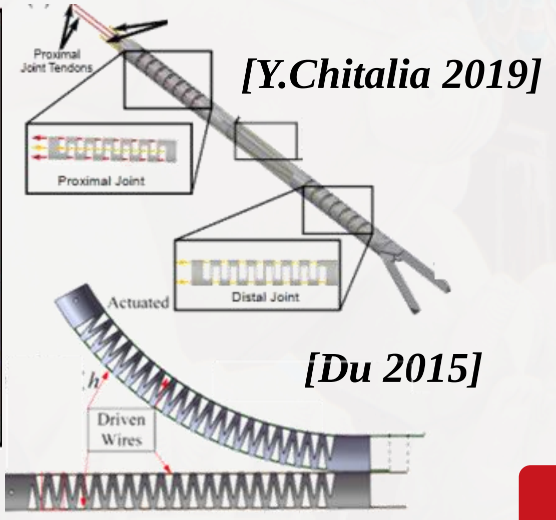

[Y.Chitalia 2019]

[Du 2015]

Requirements

Confined and unstructured spaces

Accurate position carry end effectors

Large Range of Motion ⟺ **Large Stiffness**

- Adding fillets to the corners

Large Range of Motion		Large Stiffness
↓	**Tube Diameter**	↑
↑	**Notch Depth**	↓
↑	**Section Number**	↓
↑	**Elastic strain limits**	↓

- Contact-aided
- Rolling contact

- Large tendon force
- Large strain
- Friction

⇓

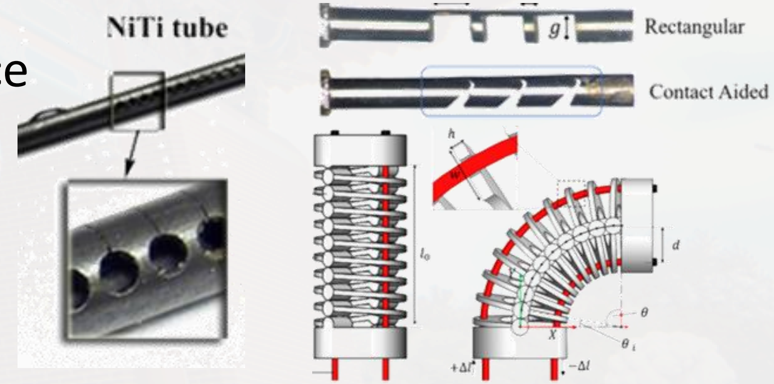

Notch Pattern Design to solve the tradeoff

1. Background: CAFP/CCAFP

Cross-Axis Flexural Pivot (CAFP)

- Beam-based Compliant Mechanism
- Low wear and friction
- Absence of backlash
- Manufactured as a single part

Bio-inspired contact-aided compliant wrist *[P. Bilancia 2021]*

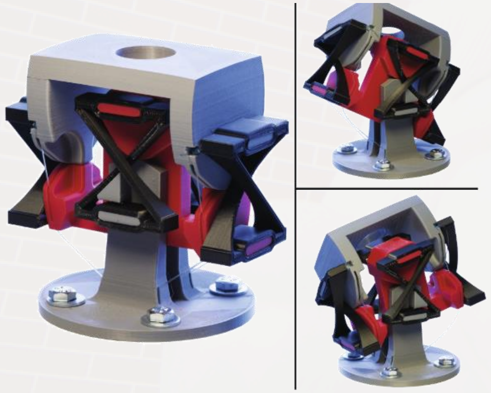

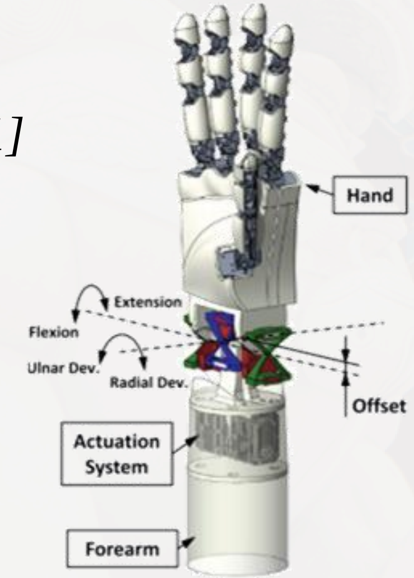

Cylindrical Cross-Axis Flexural Pivot (CCAFP)

- Integrated into a hollow shaft without interfering with internal components
- Reduce part count, simple manufacturing
- Cam-surface integrated in the cylinder

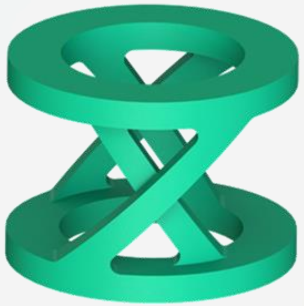

Cam-guided CCAFP for minimally invasive surgical wrist *[J. Dearden 2018]*

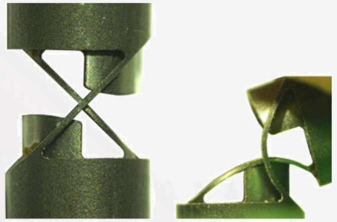

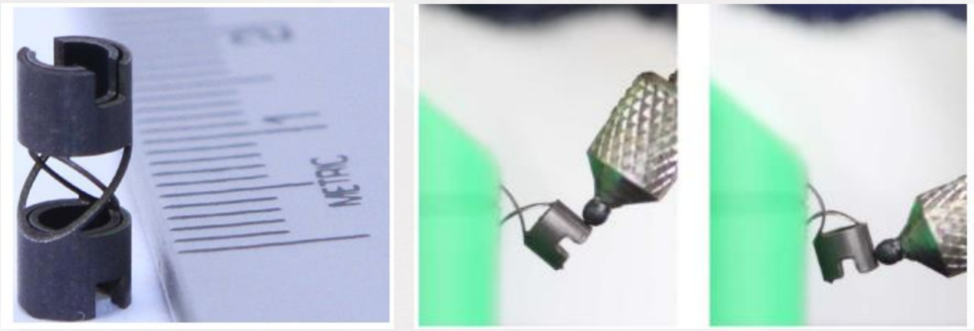

Compliant mechanisms in minimally invasive surgical applications

2.1 Design of the SCAN Manipulator

Design and Manufacture

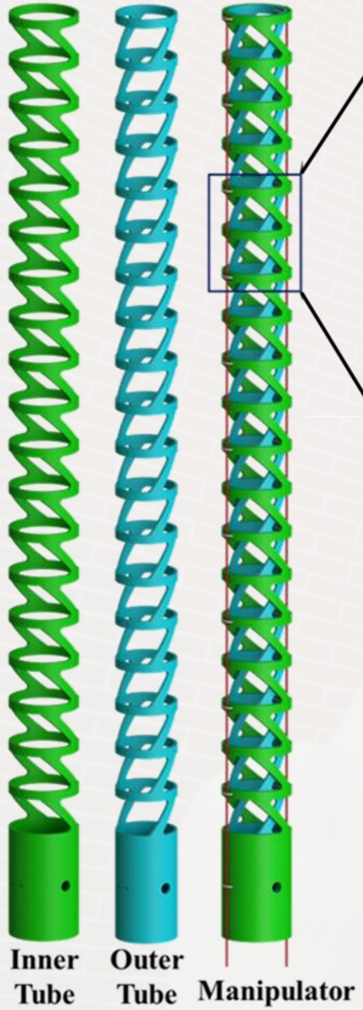

Total length: 43mm

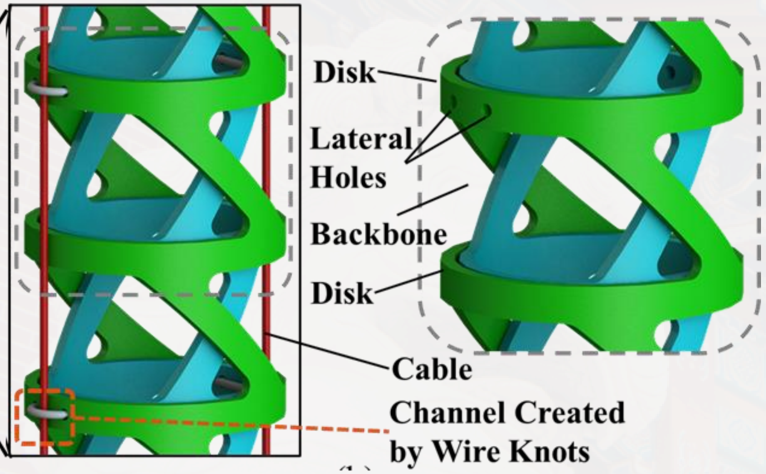

Cable Routing

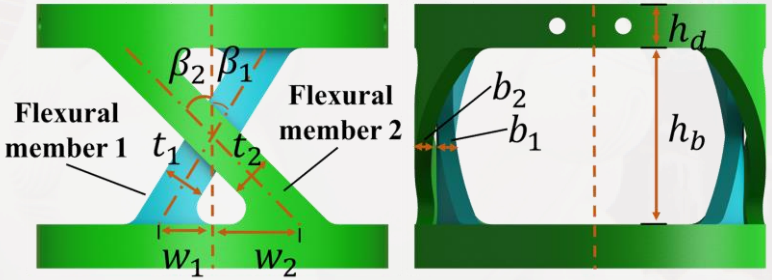

Single Section

Outer tube: OD: 3.2mm ID:2.9mm
Inner tube: OD:2.8mm ID:2.5mm

CCAFP →
- a longer bending beam length
- higher second area of inertia

1. **High axial** force stiffness
2. Stiffness transverse to the bending plane
3. Selectively alter the stiffness and range of motion by changing the crossing angle
4. **Smaller strain** to improve the safety
5. **Larger deflection** within the ultimate strain

Prototype by laser cutting

2.2 Modeling of the SCAN Manipulator

Static Model: Single Section

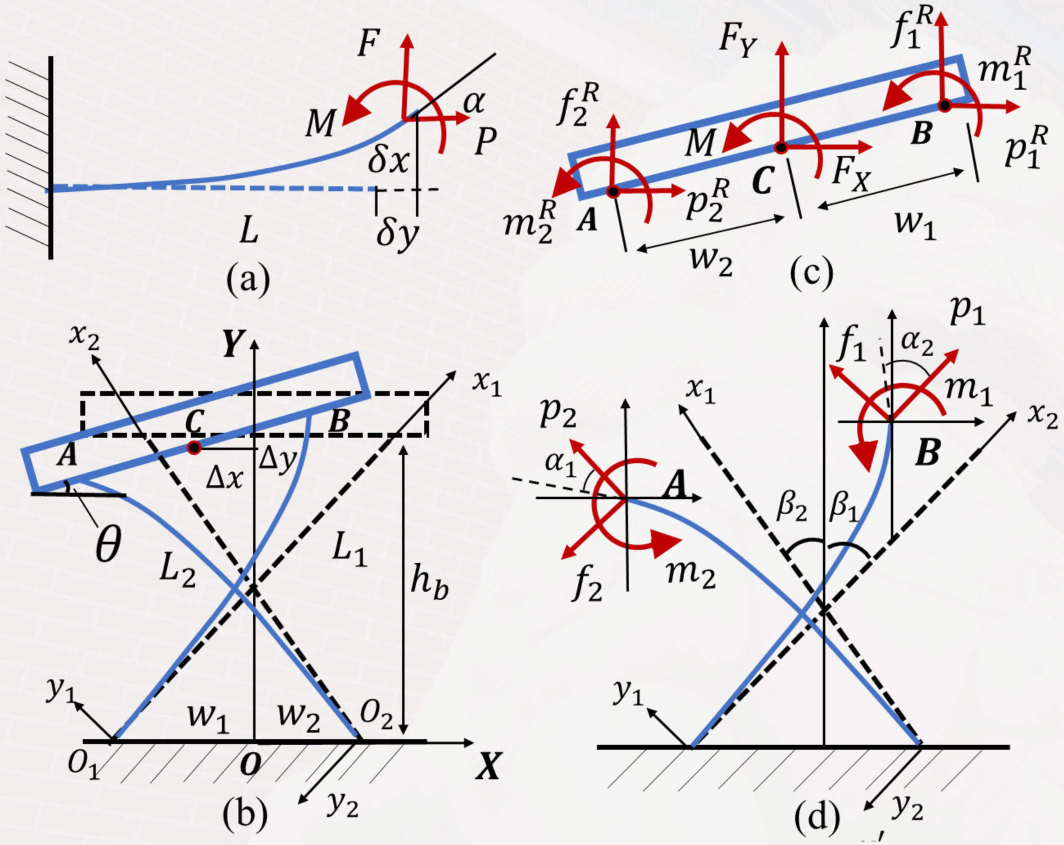

Beam-Constraint Model (BCM)

$$\begin{bmatrix} f_i \\ m_i \end{bmatrix} = G\begin{bmatrix}\delta_{yi}\\ \alpha_i\end{bmatrix} + p_i P_c \begin{bmatrix}\delta_{yi}\\ \alpha_i\end{bmatrix} + {p_i}^2 Q_c \begin{bmatrix}\delta_{yi}\\ \alpha_i\end{bmatrix}$$

$$\delta_{xi} = \frac{{t_i}^2 p_i}{12{L_i}^2} - \frac{1}{2}\begin{bmatrix}\delta_{yi}\\ \alpha_i\end{bmatrix}^T U_c \begin{bmatrix}\delta_{yi}\\ \alpha_i\end{bmatrix} - p_i \begin{bmatrix}\delta_{yi}\\ \alpha_i\end{bmatrix}^T V_c \begin{bmatrix}\delta_{yi}\\ \alpha_i\end{bmatrix}$$

Global Statics Equilibrium

$$M = (w_1 + w_2)\frac{EI_2}{L_2^2}\begin{bmatrix}\sin\theta & -\cos\theta\end{bmatrix}\begin{bmatrix}\sin\beta_2 & \cos\beta_2\\ -\cos\beta_2 & \sin\beta_2\end{bmatrix}\begin{bmatrix}p_2\\ f_2\end{bmatrix} + w_1\begin{bmatrix}\sin\theta & -\cos\theta\end{bmatrix}\begin{bmatrix}F_x\\ F_y\end{bmatrix} + \frac{EI_1}{L_1}m_1 - \frac{EI_2}{L_2}m_2$$

$$\begin{bmatrix}F_x\\ F_y\end{bmatrix} + \frac{EI_1}{L_1^2}\begin{bmatrix}-\sin\beta_1 & \cos\beta_1\\ -\cos\beta_1 & -\sin\beta_1\end{bmatrix}\begin{bmatrix}p_1\\ f_1\end{bmatrix} + \frac{EI_2}{L_2^2}\begin{bmatrix}\sin\beta_2 & \cos\beta_2\\ -\cos\beta_2 & \sin\beta_2\end{bmatrix}\begin{bmatrix}p_2\\ f_2\end{bmatrix} = 0$$

Global Geometric Constraint Equations

$$\begin{bmatrix}(w_1 + w_2) + (w_2 + w_1)\cos\theta\\ (w_1 + w_2)\sin\theta\end{bmatrix} = \begin{bmatrix}-\sin\beta_2 & -\cos\beta_2\\ \cos\beta_2 & -\sin\beta_2\end{bmatrix}\begin{bmatrix}x_A\\ y_A\end{bmatrix} - \begin{bmatrix}\sin\beta_1 & -\cos\beta_1\\ \cos\beta_1 & \sin\beta_1\end{bmatrix}\begin{bmatrix}x_B\\ y_B\end{bmatrix}$$

$$\theta = \alpha_1 = \alpha_2$$

Getting deflection $[\Delta x\ \Delta y\ \theta]$ under external load $[F_x\ F_y\ M]$

$$\begin{bmatrix}\Delta x\\ \Delta y\end{bmatrix} = \begin{bmatrix}-\sin\beta_2 & -\cos\beta_2\\ \cos\beta_2 & -\sin\beta_2\end{bmatrix}\begin{bmatrix}x_A\\ y_A\end{bmatrix} + \begin{bmatrix}w_2 + w_2\cos\theta\\ w_2\sin\theta\end{bmatrix} - \begin{bmatrix}0\\ L_2\cos\beta_2\end{bmatrix}$$

Static Model: Second moment of area

CCAFP – Elliptical Beam

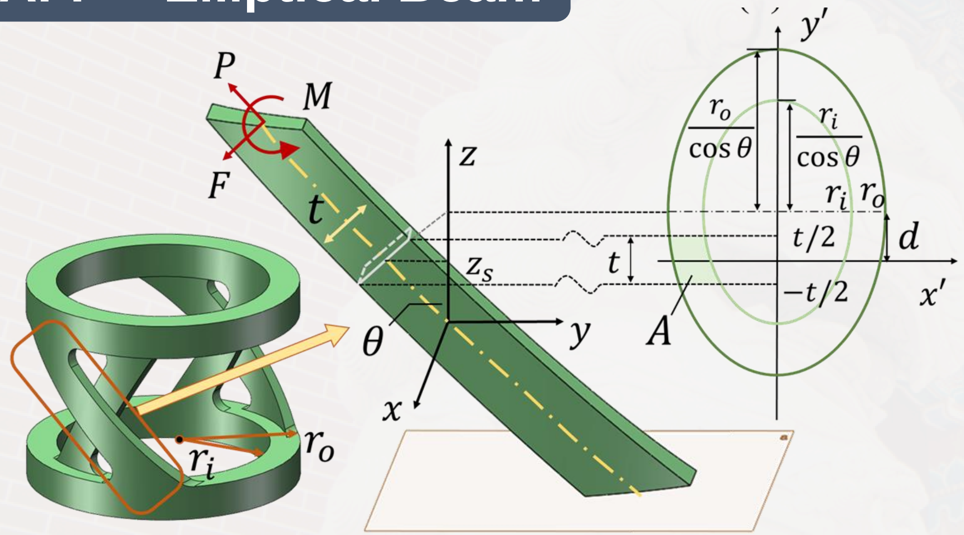

$$d = z_s \sin\theta / \cos^2\theta$$

$$I(z_s) = \int_A y'^2 \, dA = \int_{-t/2}^{t/2} y'^2 \left(\sqrt{r_o^2 - (y'\cos\theta - z_s\tan\theta)^2} - \sqrt{r_i^2 - (y'\cos\theta - z_s\tan\theta)^2} \right) dy'$$

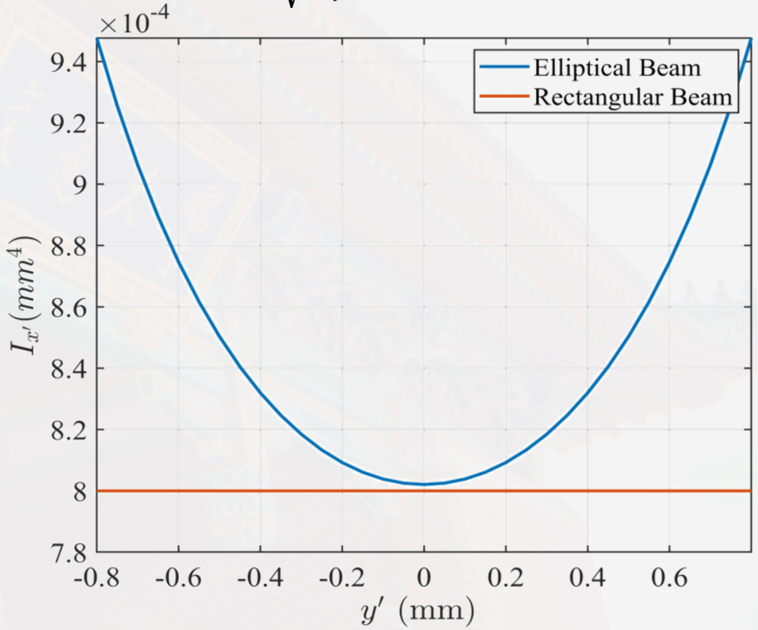

CAFP – Rectangular Beam

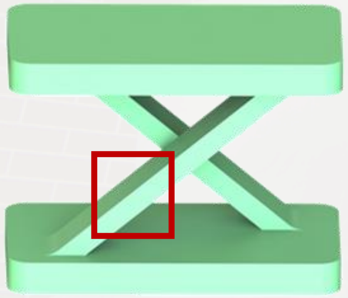

t In-plane thickness

b Out-of-plane thickness

Second moment of area $I = \frac{1}{12} t^3 b$

CCAFP's Flexure has Larger Second Moment of Area

Static Model: Multiple Section

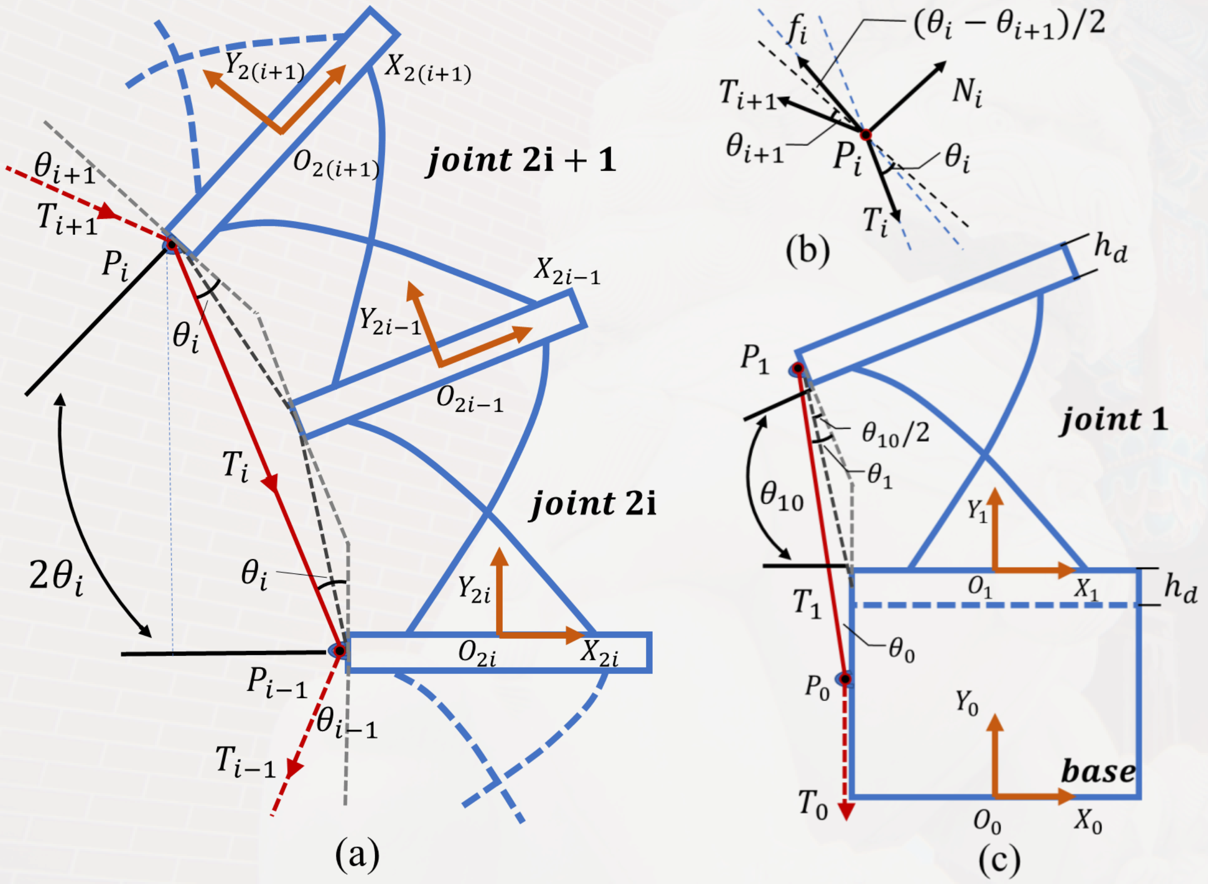

Tendon Force Propagation

$$T_{i+1} = T_i \cdot \frac{\cos\frac{\theta_i + \theta_{i+1}}{2} - \mu_i \sin\frac{\theta_i + \theta_{i+1}}{2}}{\cos\frac{\theta_i + \theta_{i+1}}{2} + \mu_i \sin\frac{\theta_i + \theta_{i+1}}{2}}$$

$$T_1 = T_0 \cdot \frac{\cos\theta_0/2 - \mu_0 \sin\theta_0/2}{\cos\theta_0/2 + \mu_0 \sin\theta_0/2}$$

Input of Single Section

$[\Delta x_i \; \Delta y_i \; \theta_i]$

$$F_{xi} = T_i \sin\frac{\theta_i}{2}, F_{yi} = -T_i \cos\frac{\theta_i}{2}, M_i = r_t T_i \cos\frac{\theta_i}{2}$$

Homogeneous transformation

$$\mathbf{A}_i^{i+1} = \begin{bmatrix} 1 & 0 & 0 & 0 \\ 0 & \cos\theta_i & -\sin\theta_i & \Delta x_i \\ 0 & \sin\theta_i & \cos\theta_i & \Delta y_i \\ 0 & 0 & 0 & 1 \end{bmatrix} \quad \mathbf{A}_G^{tip} = \mathbf{A}_0 \prod_{i=1}^{n} \mathbf{A}_i^{i+1} \mathbf{A}_d$$

Getting Manipulator's Tip Position in the Base Frame

2.3 Model Analysis and Validation

Model Analysis

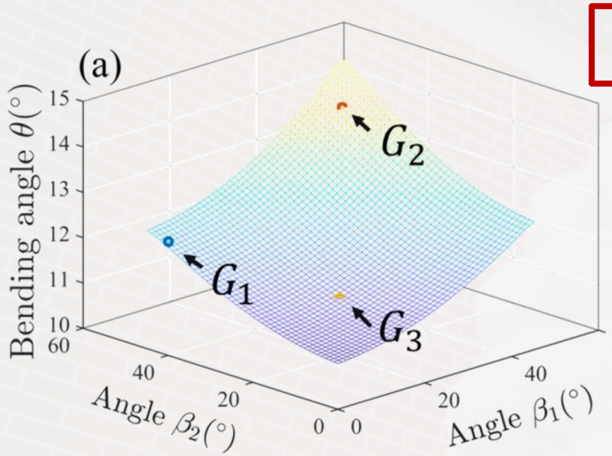

Same External Moment

Larger Crossing Angle of Cross-axis Flexures

Larger Bending Angle of the One single Joint

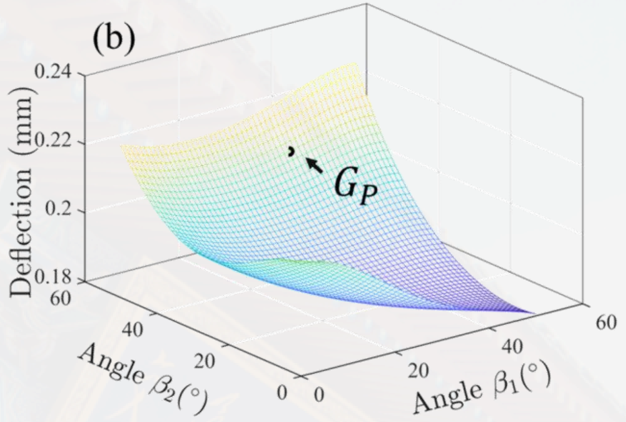

Same Lateral Force

Larger Crossing Angle of Cross-axis Flexures

Potential to Reduce Tip Deflection

Validation by Finite Element Analysis (FEA)

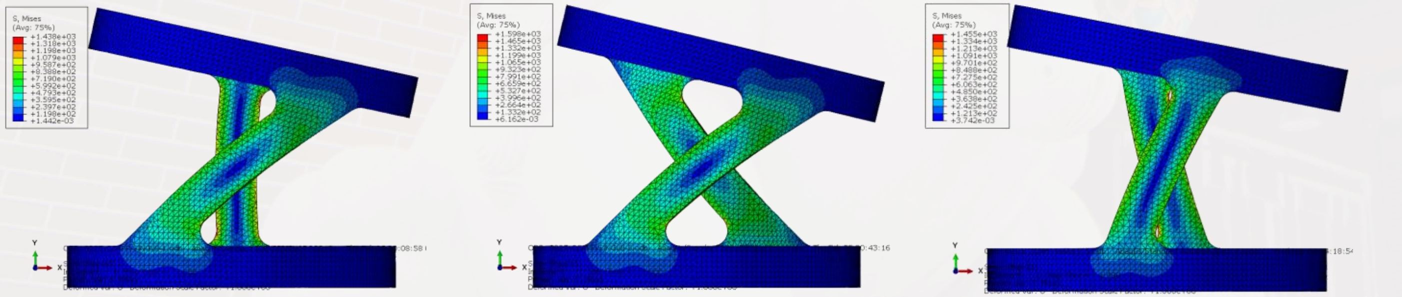

G_1: $\beta_1 = 5^\circ$, $\beta_2 = 45^\circ$ G_2: $\beta_1 = 45^\circ, \beta_2 = 45^\circ$ G_3: $\beta_1 = 20^\circ, \beta_2 = 20^\circ$

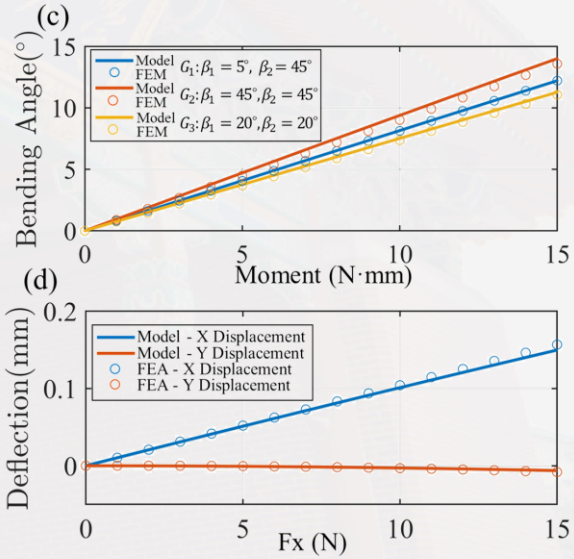

Mean Error

G1: 0.16%

G2: 2:01%

G3: 0:76%

Max error

0.0071 mm in *X*

0.0019 mm in *Y*

Improve the bending angle while ensure the stiffness

2.3 Model Analysis and Validation

Validation by FEA: Whole Manipulator

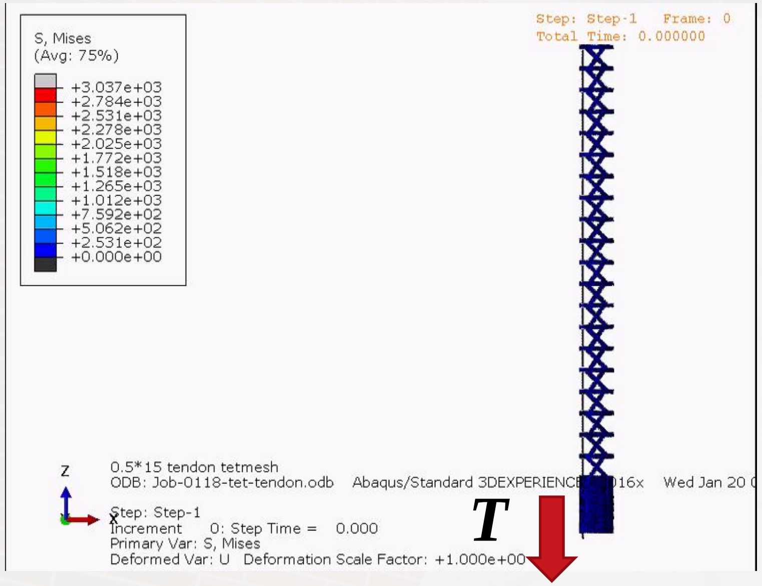

- **Under Tendon Force**
- **7.5N — 15 steps**

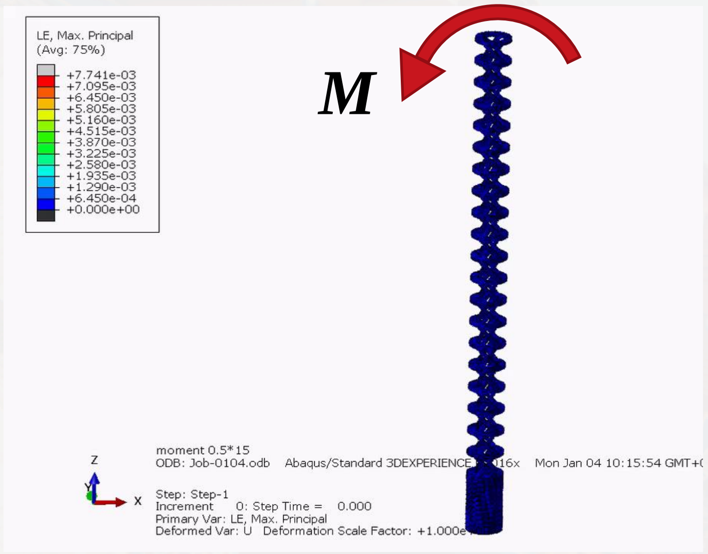

- **Under Pure Moment on Tip**
- **7.5N·mm — 15 steps**

- Friction coefficient = 0.6
- Non-constant Curvature

- Mean Tip Position Error is 0.53 mm
- 1.24% of the manipulator length

Both the shape and tip position reached a good agreement

Comparison of FEA and Theoretical Model

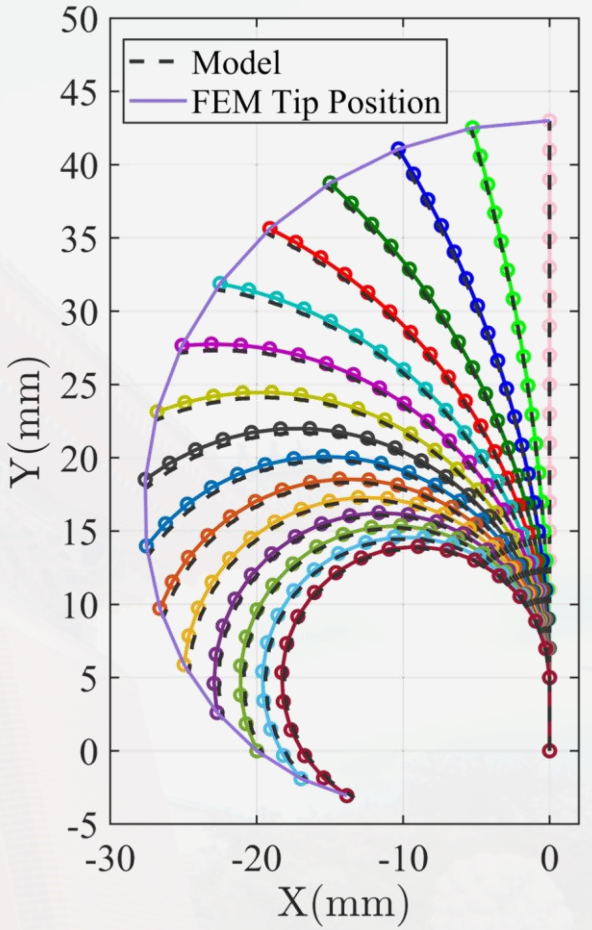

2.3 Model Analysis and Validation

FEA Result Comparison

9 N•mm pure moment applied to the tip

- 58.7° larger in bending angle
- 33.5% improvement in the range of motion

Both reaching 175° bending angle

- 28.4% smaller in max strain
- 22.45% less force to actuate

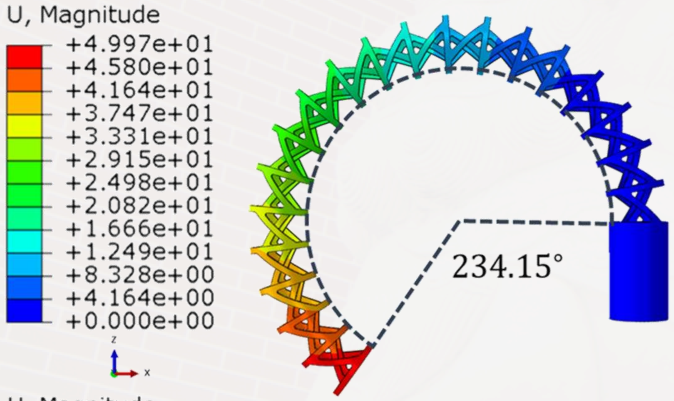

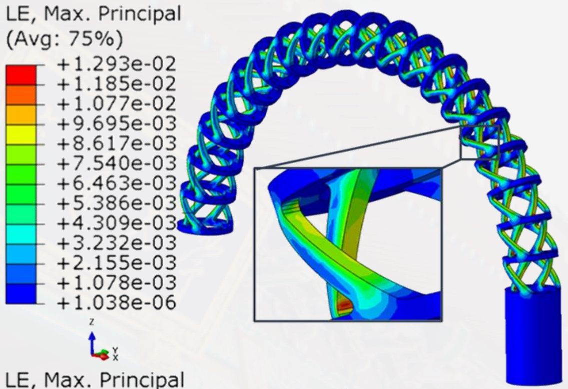

- max strain 1.293%
- 7.35 N·mm to drive

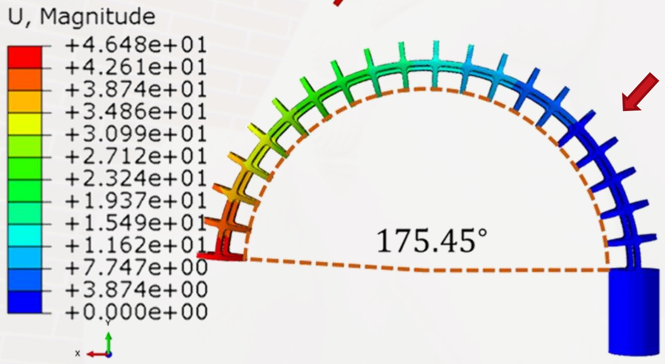

Bidirectional symmetric notched manipulator

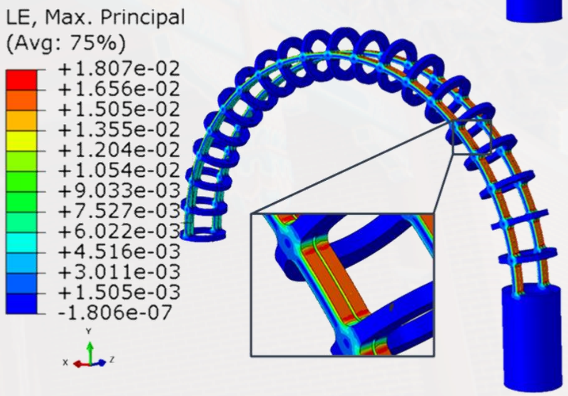

- max strain 1.807%
- 9 N·mm to drive

Superiority in strain and range of motion compared with traditional design

3.1 Experimental Setup

Actuation and Force Measurement Platform

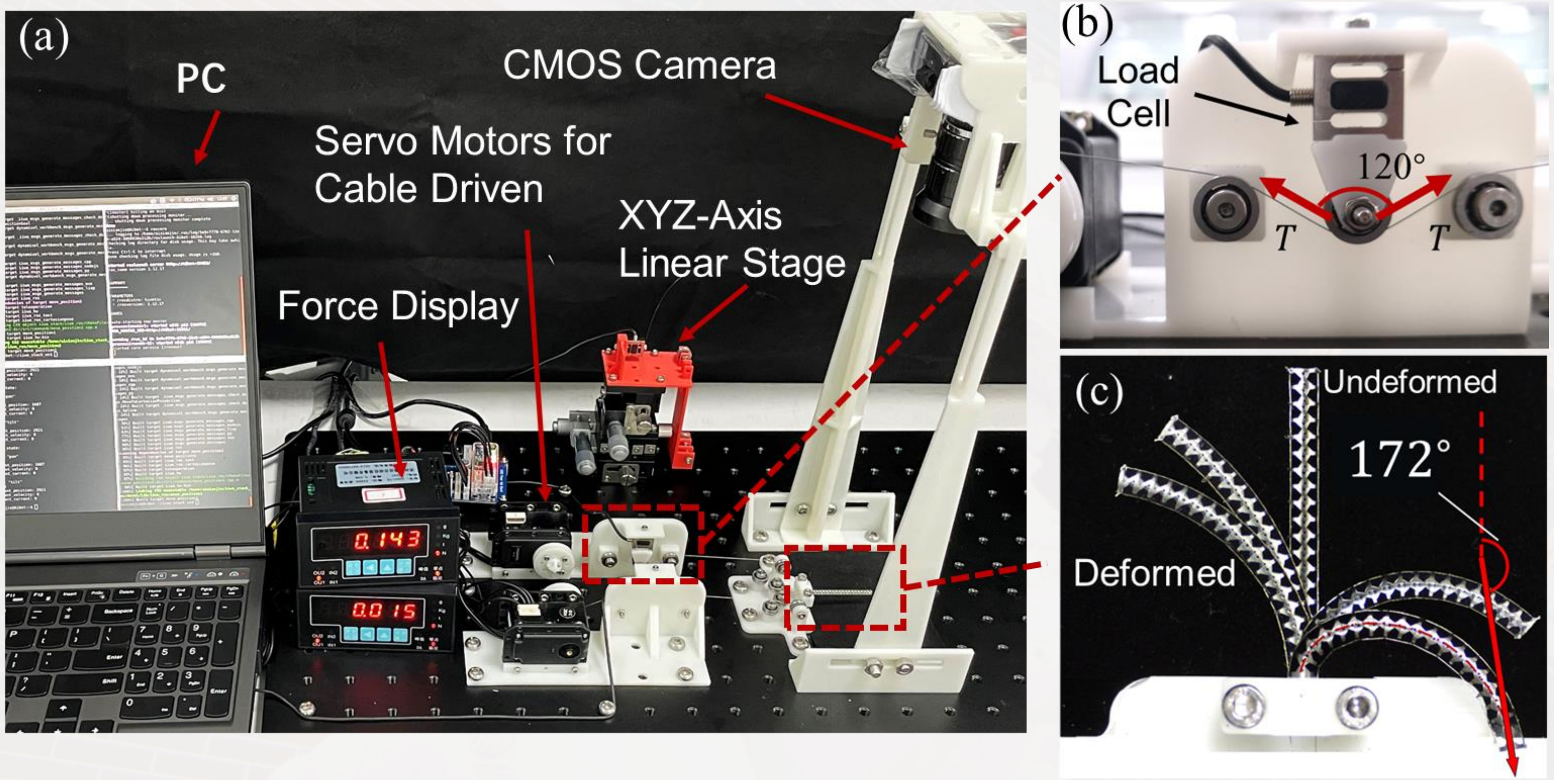

- Manipulator: nitinol tube; cable: 0.1mm stainless steel
- Two server motors pulling the cable
- Cable tension sensor integrating load cells and guide pulleys
- **Bending angle: 172◦ with 7 N cable tension**

Deflection Demo

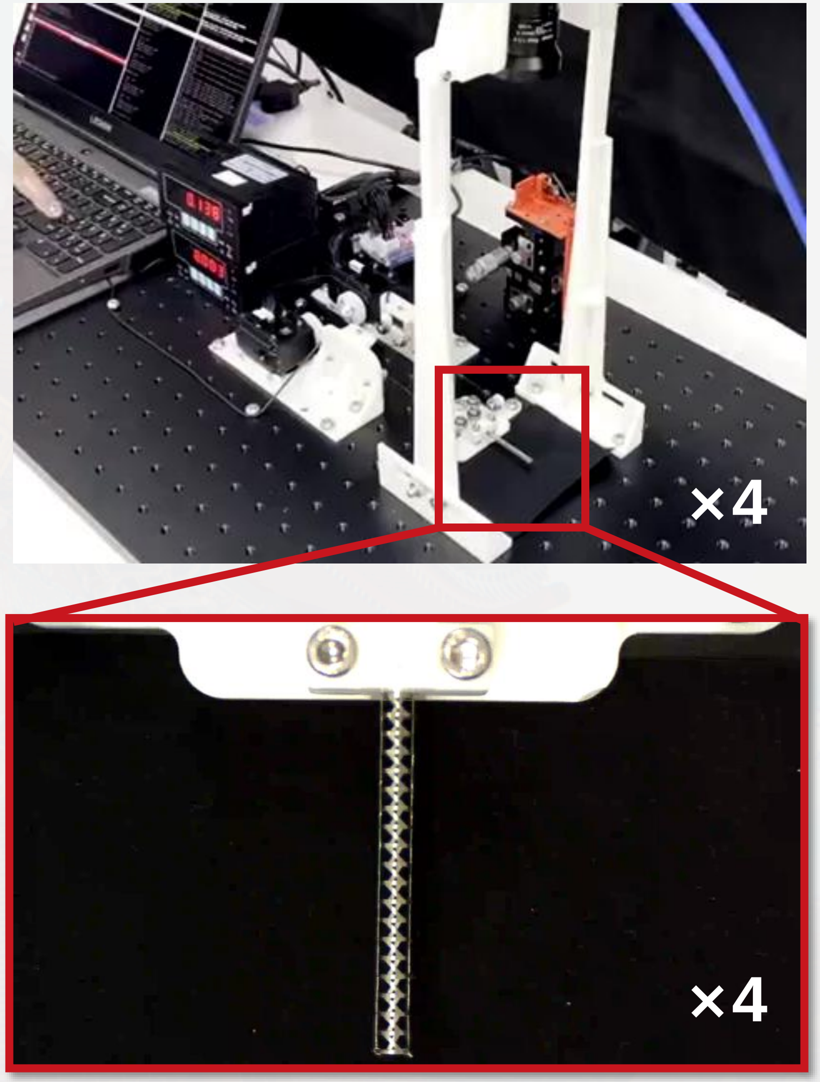

3.2 Free Bending Experiment

Evaluate the static model

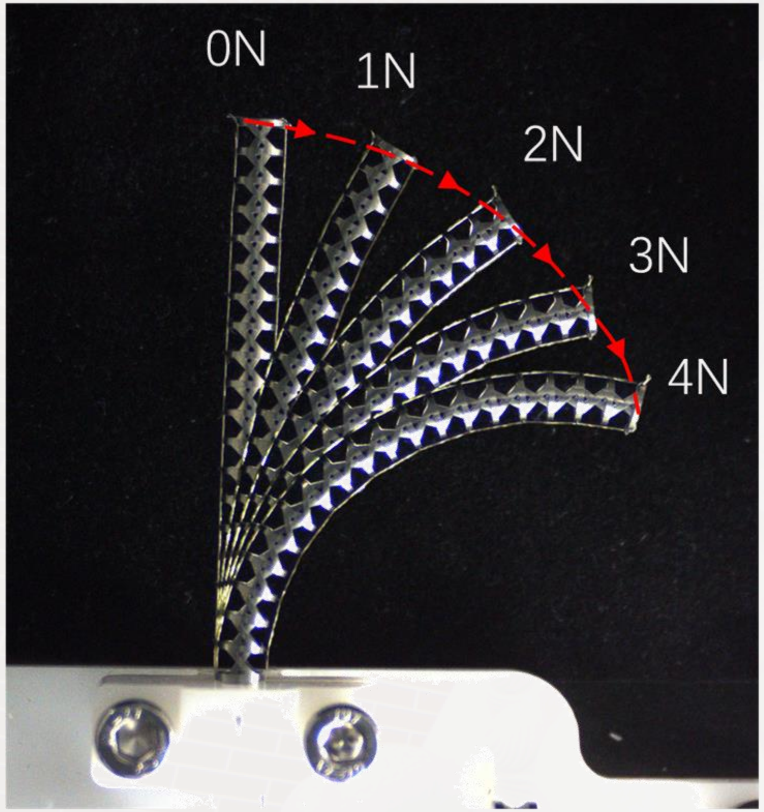

(a)

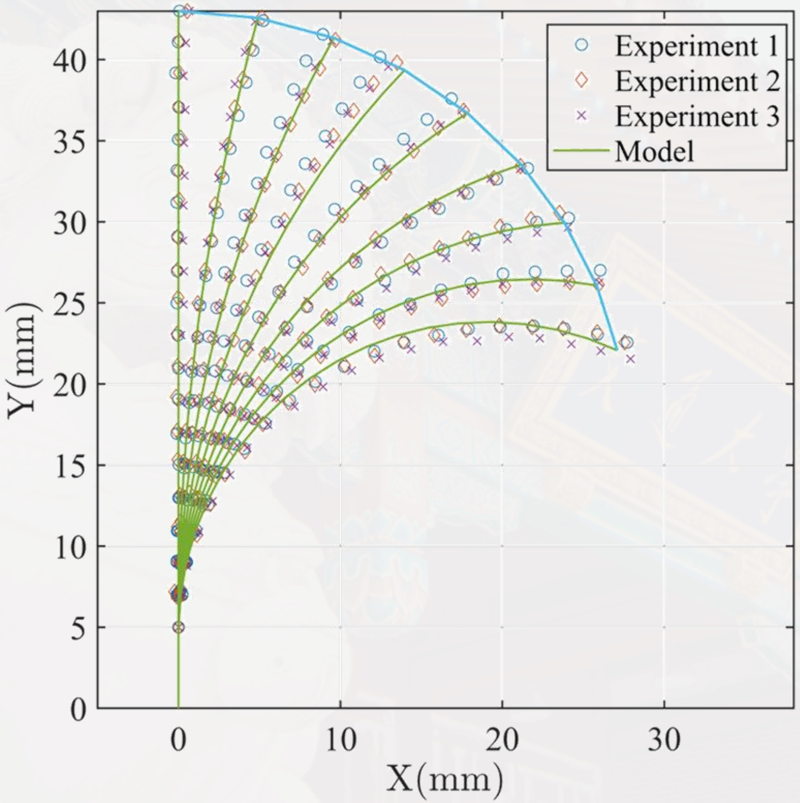

(b)

- **Calibration: identify the Young's modulus and the friction coefficient**

- Constrained optimization problem
- Sequential quadratic programming

- minimizing the estimated and the experimental tip position
- minimizing constrained nonlinear multivariable function

The mean tip error: 0.41±0.24 mm and normalization with total flexible length(38 mm): 1.074%±0.064%

Accurate static model for estimating the behavior of real manipulator

3.3 Stiffness Testing Experiment

| Lateral load to free manipulator

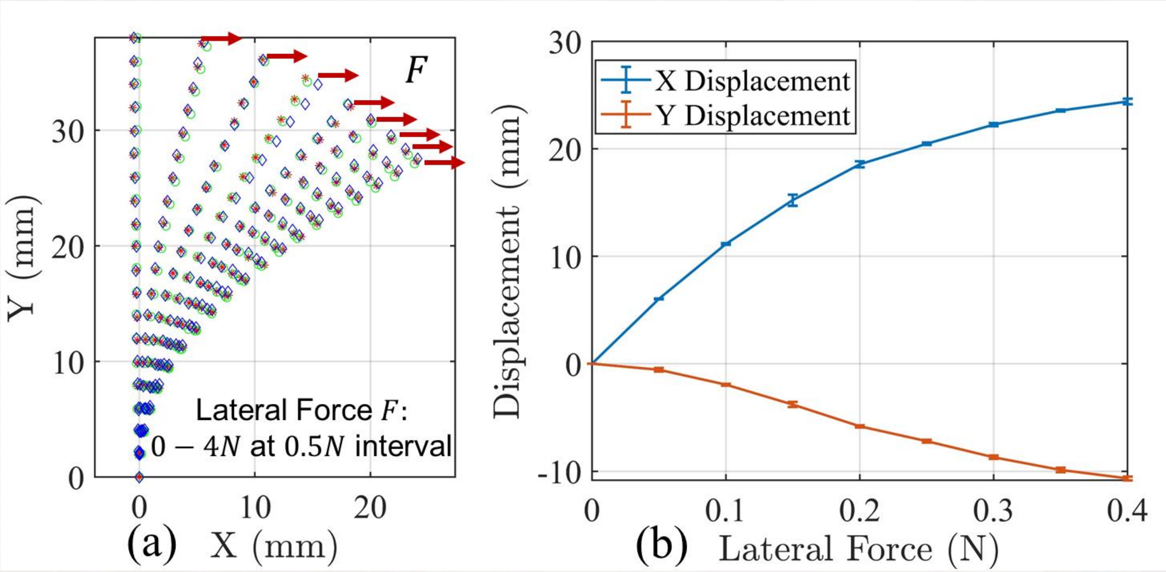

- Later force 0.4 N: 26.61 mm tip displacement
- Later force 0.3 N:
  2N cable tension — 19.95 mm tip displacement
  No cable tension — 23.87 mm tip displacement
- No significant change in X displacement with cable tension

| Lateral load with cable tension

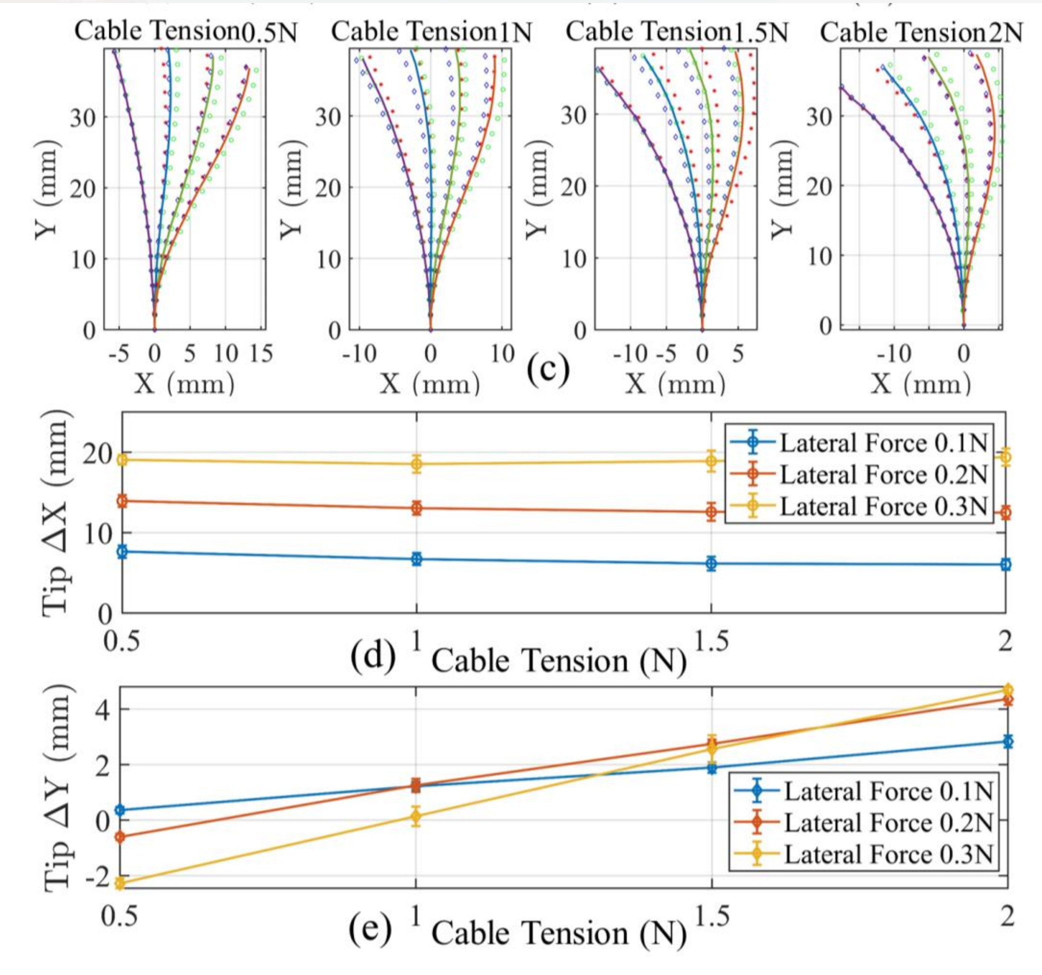

4. Discussion and Conclusion

Average curvature of one single notched section under unit actuation force κ_L

Index	Tension	Bending	Number	Length	κ_L
Bi-Asym[1]	13N	80°	14	35mm	**0.18**
Bi-Asym[2]	13N	80°	19	77.7mm	**0.08**
Ours	7N	172°	19	38mm	**0.67**

Length normalized stiffness k_L

Index	Aided	Stiffness	Length	k_L
Uni-Asym[3]	Contact-aided	13.59mm/N	6.66mm	**1.28**
Uni-Asym[3]	No contact-aided	13.59mm/N	6.66mm	**2.04**
Ours	No contact-aided	66.53mm/N	38mm	**1.75**

[1]M. D. Kutzer et al., "Design of a new cable-driven manipulator with a large open lumen: Preliminary applications in the minimally-invasive removal of osteolysis," in Proc. IEEE Int. Conf. Robot. Autom., Shanghai, China, 2011, pp. 2913–2920

[2]Z. Du et al., "Kinematics modeling of a notched continuum manipulator," *J. Mech. Robot.*, vol. 7, no. 4, Nov. 2015, Art. 041047.

[3]K. W. Eastwood et al., "Design of a contact-aided compliant notched-tube joint for surgical manipulation in confined workspaces," J. Mechanisms Robot., vol. 10, no. 1, 2018, Art. no. 015001.

Design → **Statics Modeling** → **FEA** → **Experiment**

- 33.5% larger in bending angle
- 22.45% less force to actuate
- 28.4% smaller in max strain

Future

- Task-oriented optimization
- Structure modification in cross-beams
- More elegant cable routing method

上海交通大學
SHANGHAI JIAO TONG UNIVERSITY

Thanks!

饮 水 思 源　爱 国 荣 校